MethaNet - an AI-driven approach to quantifying methane point-source emission from high-resolution 2-D plume imagery

Siraput Jongaramrungruang [1] **Christian Frankenberg** [1 2] **Andrew K. Thorpe** [2] **Georgios Matheou** [3]

Abstract

Methane (CH_4) is one of the most powerful anthropogenic greenhouse gases with a significant impact on global warming trajectory and tropospheric air quality. Quantifying an emission rate of observed CH_4 plumes from aerial or satellite images is a critical step for understanding the local distributions and subsequently prioritizing mitigation target sites. However, there exists no method that can reliably predict emission rates from detected plumes in real-time without ancillary data. Here, we trained a convolutional neural network model, called MethaNet, to predict methane point-source emission directly from high-resolution 2-D plume images without relying on other local measurements such as background wind speeds. Our results support the basis for the applicability of using deep learning techniques to quantify CH_4 point sources in an automated manner over large geographical areas. MethaNet opens the way for real-time monitoring systems, not only for present and future airborne field campaigns but also for upcoming space-based observations in this decade.

1. Introduction

Methane is the second strongest anthropogenic greenhouse gases overall in the Earth climate system. Due to its much shorter lifetime compared to that of CO_2, methane emission could be a target for emission reduction efforts to help mitigate climate impacts on a significantly shorter timescale (Montzka et al., 2011; Prather et al., 2012; Shindell et al., 2012). In fact, the 2018 NASA Decadal Survey has indicated the identification and understanding of methane emissions as one of the top priorities in the efforts to improve the future climate projection, and help lead the way in emission reduction (National Academies of Sciences, Engineering & Medicine, 2018).

Despite relatively well-constrained total global emissions, regional and local emission estimates have been challenging due to uncertainties in the process understanding and lack of sufficiently fine resolution observations that can also simultaneously cover large geographical areas. This hinders the ability to conduct mitigation efforts in the most effective manner since policy and remedy actions often take place at regional and local scales. Improved measurements of localized CH_4 point sources (e.g. 10 - 100 m scale) are integral to this effort.

One potential to fill this gap is remote-sensing imaging absorption spectrometry. This technique has opened the way for quantitative CH_4 measurements at sufficiently high resolution needed to differentiate various local sources over large areas at regional scale (Duren et al., 2019; Frankenberg et al., 2016). Using absorption features of CH_4 in the short-wave infrared around 2.3 μm, column integrated CH_4 concentration can be retrieved at a spatial resolution as fine as 1 m, allowing for the detection of CH_4 point sources from airborne spectrometers such as the next-generation Airborne Visible/Infrared Imaging Spectrometer (AVIRIS-NG) (Thorpe et al., 2017). Studies have utilized this technique for several field campaigns in the Western U.S. where more than 500 strong point sources have been detected (Duren et al., 2019; Frankenberg et al., 2016). Figure 1 shows examples of representative methane plumes from different sectors. Sources of various emission rates observed under varying wind speeds would lead to a diverse set of plume spatial distributions. Despite the progress in the detection algorithm of methane plumes, high uncertainties still exist in converting the observed concentration fields to source flux rates.

Many flux inversion methods have been proposed such as the Gaussian plume inversion (Bovensmann et al., 2010; Krings et al., 2013), source pixel estimate (Jacob et al., 2016), cross-sectional flux estimate (Cambaliza et al., 2015; 2014; Conley et al., 2016), and residence time of methane

[*]Equal contribution [1]Division of Geological and Planetary Sciences, California Institute of Technology, Pasadena, CA, USA [2]NASA Jet Propulsion Laboratory, California Institute of Technology, Pasadena, CA, USA [3]Department of Mechanical Engineering, University of Connecticut, Storrs, CT, USA. Correspondence to: Siraput Jongaramrungruang <siraput@caltech.edu>.

Proceedings of the 38^{th} International Conference on Machine Learning, PMLR 139, 2021.

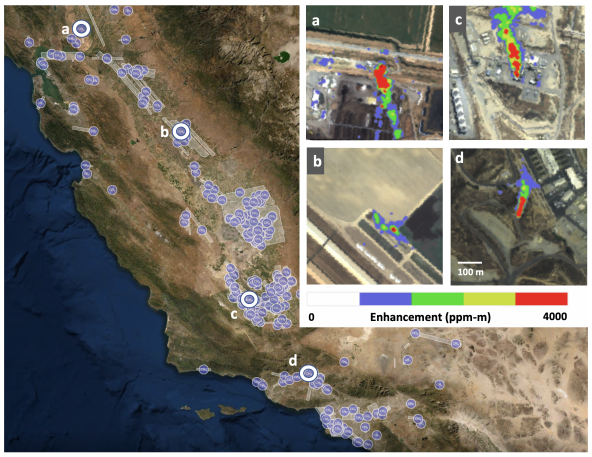

Figure 1. A map showing detected methane sources from the California Methane Source Finder project. Background image shows AVIRIS-NG flight lines conducted in 2016 and 2017 (white stripes) and locations of detected CH_4 sources (purple circles). The inset images show examples of methane plume enhancement from AVIRIS-NG observations over (a) a landfill, (b) diary manure area, (c) an oil and gas facility, and (d) a natural gas storage field.

plume enhancement (Duren et al., 2019; Varon et al., 2018). All of these techniques, however, require the knowledge of local wind speed. This hinders fast and accurate flux inversions since in situ wind measurements cannot be planned when the location of the plume is not known a priori. Due to these limitations, accurate and fast flux inversions of point sources have been challenging. Jongaramrungruang et al. (2019) tackled this challenge by utilizing plume morphology to constrain corresponding wind speed and thus flux rate. It provides evidence that the morphology of methane plumes, as observed from remote sensing images, contains useful information about the background wind speed during the flight overpass, which, in turn, is a critical component of predicting accurate flux estimates. In that work, a plume angular width is constructed as a simple metric to represent the geometry of observed methane plumes. Essentially, the 2D pattern of the plume is simply reduced into one dimension, which was an ad hoc choice. However, the full spatial structure of the plume morphology can potentially be utilized such that emission rates are predicted at even higher accuracy, as well as in a more automated and objective manner.

Modern machine learning techniques are designed for problems as this task. Convolutional Neural Network (CNN) is a model architecture that has shown tremendous success in image recognition tasks (He et al., 2016; Krizhevsky et al., 2012; Simonyan & Zisserman, 2015; Szegedy et al., 2014). It has been shown to be capable of learning relevant spatial patterns from an image with location invariant features similar to how a human brain understands an image. Here in this work, we build a customized CNN model and apply it to a large training dataset derived from Large Eddy Simulation (LES) (Matheou et al., 2014) output and realistic background noise over agricultural, desert and urban environments. We train our model, named MethaNet, to predict flux rates directly from 2D methane plume images. To our knowledge, this is the first time that CNN has been used for a regression task to quantify methane plume emission from 2D high-resolution imagery.

Section 2 illustrates the method on preparing the dataset, and the details on MethaNet CNN architecture. Model performance and error analyses are provided in Section 3, followed by concluding remarks in the final section.

2. Methodology

2.1. Data

To train a model capable of quantifying an emission rate from a given 2D image, a realistic modelling of CH_4 plumes is a prerequisite, as the actual plume observations with known flux rates are extremely limited. The training data is a set of simulated plume images, each with one channel representing CH_4 concentration and each has a source emission rate as a label. The LES is used to generate the time-resolved three-dimensional CH_4 distribution in the boundary layer, over a range of 1-10 m/s wind speeds. This enables a realistic simulation of how methane concentrations from a point source evolve in space, given various background wind speeds and source flux rates. The full description of the LES model setup can be found in Jongaramrungruang et al. (2019).

This allows us to efficiently create synthetic plumes originating from sources spanning orders of magnitudes in flux rates. In this work, we focus on plume emission rates between 0 and 2000 kg/hr which is the range in which the majority of typical methane point sources were observed (Duren et al., 2019). Each of these 2D images is then augmented by continuous random rotation between -170° to 170° and translation between -30 to +30 pixels, to generate a diverse set of possible plume orientations and center locations. Additionally, superposed on each an image is a noise matrix with the same size as the plume image. The illustration of this synthetic plume generation is shown in Figure 2. The noise matrix is taken from retrieval background variations from actual AVIRIS-NG scenes in the absence of plumes. In our work, we obtained scenes over a variety of surfaces, including urban, desert, and agricultural areas.

Building a successful neural network model generally requires large data samples. These data are separated into training, validation and test sets that share a similar distribution but are distinct from one another. Our training data is

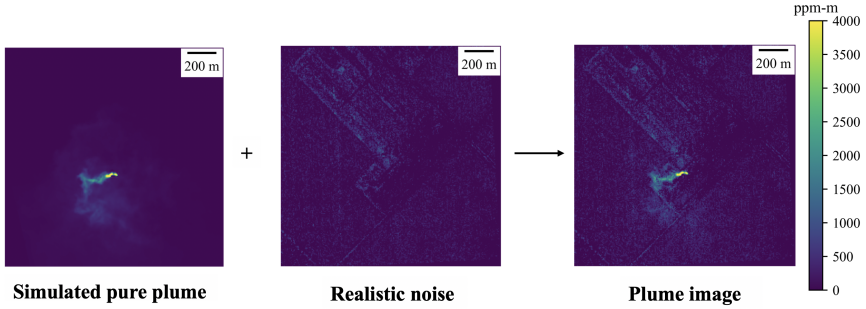

Figure 2. An example of a plume image from a simulated plume superposed on a realistic retrieval noise background based on an AVIRIS-NG observation over agricultural area.

a set images of plumes of different sizes and shapes under various wind speeds and background noise. In our study, we assign images from independent LES runs for training, validation and test sets (300K, 10K, and 3K samples respectively). We also assign background noise scenes into three buckets, each to be used exclusively in each of the three sets to ensure no data contamination among them. After MethaNet is trained, validated, and tested in the simulation world, the best model is also applied to make a prediction on a few available actual plume observations from a ground controlled-release experiment.

2.2. Model

Machine learning methods have been used extensively in many fields to predictive problems. One particular model in machine learning that has found a great success in computer vision tasks is CNN (He et al., 2016; Krizhevsky et al., 2012; Simonyan & Zisserman, 2015; Szegedy et al., 2014). It has been the primary building blocks for tasks such as face recognition, image classification, autonomous driving. Because of its versatility, recently it has been adopted in tackling environmental science-related problems such as gas leak classification and wild fire classification based on remote-sensing images (Kumar et al., 2020; Pan et al., 2020; Wang et al., 2020). However, most of the CNN applications in environmental science has been primarily limited to a classification problem. Here, for the first time, we applied CNN to predict methane quantification directly from a 2D image as a regression task. We develop a customized CNN model, named MethaNet, based on a basic building block where a convolutional layer with a non-linear activation function is followed by a max pooling layer, then combining with a few fully-connected layers before the last output layer that determines the flux rate a scalar value.

In our case, an image dimension of 300*300 pixels is suitable, as it covers a range of 1.5*1.5 km^2, which can fully capture typical plume dimensions of less than 1 km. The input image has only 1 channel representing a value of retrieved CH_4 enhancement (this value is not bounded by 255 as typical in RGB). The architecture consists of a series of convolutional layers each with different numbers of filters and sizes, and each has a Rectified Linear Unit (ReLu) activation function. Max pooling layers are also applied after certain convolutional layers, and a dropout layer is included as a regularization to reduce overfitting. After these combined layers, the output is then flattened and passed to fully-connected layers with 64 and 32 neurons with ReLU activations. Finally, the output layer contains one neuron with a scaler output for a regression task to quantify methane emission rate from the input image.

3. Results and Analysis

In this section, we show the performance of MethaNet on predicting methane emission rates. The comparison between the true and predicted fluxes from the test set are shown in Figure 3. A key metric that is widely used to characterize the effectiveness of plume emission estimates in the field is the mean absolute percentage error.

Generally, MethaNet predictions align well with the true values as indicated by the concentration of points close to the 1:1 line. For plumes with emission rates above 40 kg/hr, our model can predict with the mean absolute percentage error of under 17%.

We see some outliers for some plumes at very low fluxes, especially under 30 kg/hr. Inspection on the data points with low fluxes and high prediction error reveals that these scenes have bright surface features (high correlated noise levels), which interfere with how the network perceives and predict the actual fluxes from the images. For these scenes, it is hard for even human eyes to distinguish plumes from the noise. Thus, it is hard for the model to perform well on scenes in such an extreme case. Predictions for plumes under high background wind speeds (8-10 m/s) also tend to underestimate the true flux rates. This could be because plumes have more elongated structures under such high wind speeds; these structures were seen less often in the training data compared to typical more-rounded structures

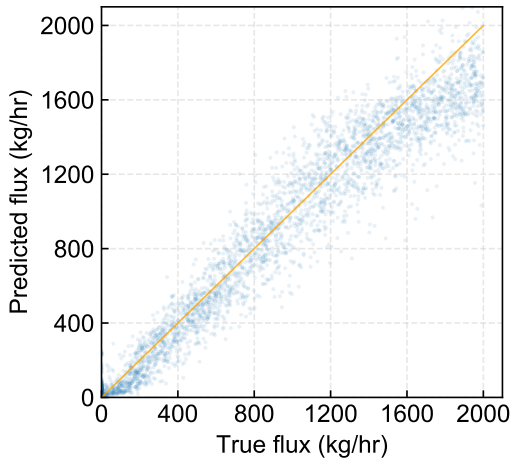

Figure 3. A plot showing a comparison between true fluxes and predicted fluxes by MethaNet trained from all LES runs with realistic background noise to predict unseen plumes in test set. A solid line shows a 1:1 relationship.

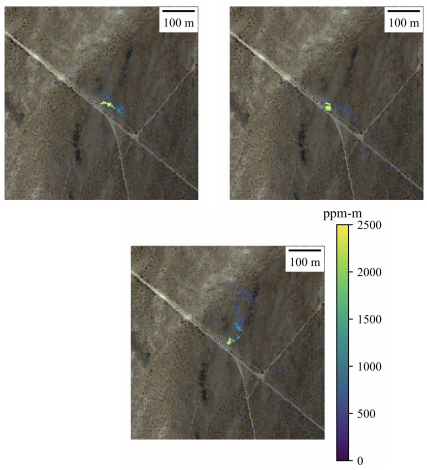

Figure 4. Controlled release experiment conducted at Victorville, CA. The scenes represent 3 overpasses with a controlled flux rate of 39 kg/hr. The enhancement in color is used for MethaNet input; the background RGB is shown only for visual reference.

under lower wind speed regimes. Overall, it is evident that our model can predict the emission rate of methane plumes accurately without the need for wind speed information. Over the same range of flux rates, this level of accuracy surpasses other previous methods, which even require wind speeds to estimate emission rates. This is a significant part in deploying the model for a real-time application during field campaigns and future monitoring systems. This level of performance at a mean absolute percentage error of 17% is a state-of-the-art achievement for a model that does not even rely on wind speed information.

To further demonstrate the validity of this method, we apply our model to actual 2D scenes of a methane plume from a controlled-release experiment from a natural gas pipeline located at Victorville, CA (34.8, -117.3), on 15-17 June, 2017, with a flux release of 39 ± 5 kg/hr. The three snapshots of the same plume from this source is shown in Figure 4. Based on each snapshot, we feed the 2D image into our trained model and directly obtain a prediction of emission rate of the source. The predicted flux rates are 33, 26, and 32 kg/hr. The mean and standard deviation is 31 and 3, respectively. This is consistent with the actual rate within one standard deviation. The mean prediction is approximately 20% deviated from the true value.

4. Conclusion

In this study, we demonstrated a novel approach using deep learning to quantify methane gas emission based on high-resolution airborne imagery. Our method demonstrates that an accurate estimate of methane emission rates can be obtained directly from CH_4 enhancement image without the need of simultaneous wind speed measurement. We build a Convolutional Neural Network model to learn the mapping between 2D plume images and theirs corresponding source emission rates under various wind speed conditions. The training data are derived from realistic plume simulation using LES and realistic retrieval noise from AVIRIS-NG field observations. Our simulated CH_4 images represent a diverse set of realistic plumes of various emission rates between 0-2000 kg/hr in different landscape ranging from urban, desert to agriculture areas. Our error analysis based on the model prediction of a hold-out set of unseen scenes shows an error of around 17% on average. This level of error is a significant improvement from other pre-existing approaches, while it completely removes the dependence on meteorological wind speed data which might not be reliable or available at high spatial resolution everywhere on the globe. An independent test on a controlled release experiment data over Victorville, CA, also validates a consistent prediction performance for MethaNet in real observations. We have shown that this model can be applied to quantifying methane point-source emission in a quick and automated manner based directly on plume images alone. While the range of methane emissions prescribed in this study was between 0 and 2000 kg/hr, we believe that the same approach can be applied to plumes with even higher fluxes as the plume enhancement in such case will be even more prominent compared to the surrounding noise background. With the level of performance of MethaNet, we believe it could be applied to recent large-scale flight campaigns to improve previous emission rate estimates. This also has immediate implications for future aerial campaigns and space-baed observations from anticipated satellites that will be launched in this decade.

References

Bovensmann, H., Buchwitz, M., Burrows, J. P., Reuter, M., Krings, T., Gerilowski, K., Schneising, O., Heymann, J., Tretner, A., and Erzinger, J. A remote sensing technique for global monitoring of power plant CO 2 emissions from space and related applications. *Atmospheric Measurement Techniques*, 3(4):781–811, 2010. ISSN 18671381. doi: 10.5194/amt-3-781-2010.

Cambaliza, M. O., Shepson, P. B., Caulton, D. R., Stirm, B., Samarov, D., Gurney, K. R., Turnbull, J., Davis, K. J., Possolo, A., Karion, A., Sweeney, C., Moser, B., Hendricks, A., Lauvaux, T., Mays, K., Whetstone, J., Huang, J., Razlivanov, I., Miles, N. L., and Richardson, S. J. Assessment of uncertainties of an aircraft-based mass balance approach for quantifying urban greenhouse gas emissions. *Atmospheric Chemistry and Physics*, 14(17):9029–9050, 2014. ISSN 16807324. doi: 10.5194/acp-14-9029-2014.

Cambaliza, M. O., Shepson, P. B., Bogner, J., Caulton, D. R., Stirm, B., Sweeney, C., Montzka, S. A., Gurney, K. R., Spokas, K., Salmon, O. E., Lavoie, T. N., Hendricks, A., Mays, K., Turnbull, J., Miller, B. R., Lauvaux, T., Davis, K., Karion, A., Moser, B., Miller, C., Obermeyer, C., Whetstone, J., Prasad, K., Miles, N., and Richardson, S. Quantification and source apportionment of the methane emission flux from the city of Indianapolis. *Elementa*, 3:1–18, 2015. ISSN 23251026. doi: 10.12952/journal.elementa.000037.

Conley, S., Franco, G., Faloona, I., Blake, D. R., Peischl, J., and Ryerson, T. B. Methane emissions from the 2015 Aliso Canyon blowout in Los Angeles, CA. *Science*, 351 (6279):1317–1320, 2016. ISSN 10959203. doi: 10.1126/science.aaf2348.

Duren, R. M., Thorpe, A. K., Foster, K. T., Rafiq, T., Hopkins, F. M., Yadav, V., Bue, B. D., Thompson, D. R., Conley, S., Colombi, N. K., Frankenberg, C., McCubbin, I. B., Eastwood, M. L., Falk, M., Herner, J. D., Croes, B. E., Green, R. O., and Miller, C. E. California's methane super-emitters. *Nature*, 575(7781): 180–184, 2019. ISSN 14764687. doi: 10.1038/s41586-019-1720-3. URL http://dx.doi.org/10.1038/s41586-019-1720-3.

Frankenberg, C., Thorpe, A. K., Thompson, D. R., Hulley, G., Kort, E. A., Vance, N., Borchardt, J., Krings, T., Gerilowski, K., Sweeney, C., Conley, S., Bue, B. D., Aubrey, A. D., Hook, S., and Green, R. O. Airborne methane remote measurements reveal heavy-tail flux distribution in Four Corners region. *Proceedings of the National Academy of Sciences*, 113(35):9734–9739, 2016. ISSN 0027-8424. doi: 10.1073/pnas.1605617113. URL http://www.pnas.org/lookup/doi/10.1073/pnas.1605617113.

He, K., Zhang, X., Ren, S., and Sun, J. Deep residual learning for image recognition. *Proceedings of the IEEE Computer Society Conference on Computer Vision and Pattern Recognition*, 2016-Decem:770–778, 2016. ISSN 10636919. doi: 10.1109/CVPR.2016.90.

Jacob, D., Turner, A., Maasakkers, J., Sheng, J., Sun, K., Liu, X., Chance, K., Aben, I., McKeever, J., and Frankenberg, C. Satellite observations of atmospheric methane and their value for quantifying methane emissions. *Atmospheric Chemistry and Physics*, 16(22), 2016. ISSN 16807324. doi: 10.5194/acp-16-14371-2016.

Jongaramrungruang, S., Frankenberg, C., Matheou, G., Thorpe, A., Thompson, D., Kuai, L., and Duren, R. Towards accurate methane point-source quantification from high-resolution 2-D plume imagery. *Atmospheric Measurement Techniques*, 12(12), 2019. ISSN 18678548. doi: 10.5194/amt-12-6667-2019.

Krings, T., Gerilowski, K., Buchwitz, M., Hartmann, J. M., Sachs, T., Erzinger, J., Burrows, J. P., and Bovensmann, H. Quantification of methane emission rates from coal mine ventilation shafts using airborne remote sensing data. *Atmospheric Measurement Techniques*, 6(1):151–166, jan 2013. URL http://www.atmos-meas-tech.net/6/151/2013/http://file//localhost(null)papers3://publication/doi/10.5194/amt-6-151-2013.

Krizhevsky, B. A., Sutskever, I., and Hinton, G. E. ImageNet Classification with Deep Convolutional Neural Networks. *Communications of the ACM*, 60(6):84–90, 2012.

Kumar, S., Torres, C., Ulutan, O., Ayasse, A., Roberts, D., and Manjunath, B. S. Deep remote sensing methods for methane detection in overhead hyperspectral imagery. *Proceedings - 2020 IEEE Winter Conference on Applications of Computer Vision, WACV 2020*, pp. 1765–1774, 2020. doi: 10.1109/WACV45572.2020.9093600.

Matheou, G., Chung, D., Matheou, G., and Chung, D. Large-Eddy Simulation of Stratified Turbulence. Part II: Application of the Stretched-Vortex Model to the Atmospheric Boundary Layer. *Journal of the Atmospheric Sciences*, 71(12):4439–4460, dec 2014. ISSN 0022-4928. doi: 10.1175/JAS-D-13-0306.1. URL http://journals.ametsoc.org/doi/abs/10.1175/JAS-D-13-0306.1.

Montzka, S. A., Krol, M., Dlugokencky, E., Hall, B., and Jo, P. Small Interannual Variability of. *Science*, 331 (January):67–69, 2011.

National Academies of Sciences, Engineering and Medicine. Thriving on Our Changing Planet: A Decadal Strategy for

Earth Observation from Space. *The National Academies Press.*, 2018. doi: 10.17226/24938.

Pan, H., Badawi, D., and Cetin, A. E. Computationally efficient wildfire detection method using a deep convolutional network pruned via fourier analysis. *Sensors (Switzerland)*, 20(10), 2020. ISSN 14248220. doi: 10.3390/s20102891.

Prather, M. J., Holmes, C. D., and Hsu, J. Reactive greenhouse gas scenarios: Systematic exploration of uncertainties and the role of atmospheric chemistry. *Geophysical Research Letters*, 2012. ISSN 00948276. doi: 10.1029/2012GL051440.

Shindell, D., Kuylenstierna, J. C., Vignati, E., Van Dingenen, R., Amann, M., Klimont, Z., Anenberg, S. C., Muller, N., Janssens-Maenhout, G., Raes, F., Schwartz, J., Faluvegi, G., Pozzoli, L., Kupiainen, K., Höglund-Isaksson, L., Emberson, L., Streets, D., Ramanathan, V., Hicks, K., Oanh, N. T., Milly, G., Williams, M., Demkine, V., and Fowler, D. Simultaneously mitigating near-term climate change and improving human health and food security. *Science*, 335(6065):183–189, 2012. ISSN 10959203. doi: 10.1126/science.1210026.

Simonyan, K. and Zisserman, A. Very deep convolutional networks for large-scale image recognition. *3rd International Conference on Learning Representations, ICLR 2015 - Conference Track Proceedings*, pp. 1–14, 2015.

Szegedy, C., Vanhoucke, V., Shlens, J., and Wojna, Z. Rethinking the Inception Architecture for Computer Vision. *CoRR*, abs/1512.00567, 2014.

Thorpe, A. K., Frankenberg, C., Thompson, D. R., Duren, R. M., Aubrey, A. D., Bue, B. D., Green, R. O., Gerilowski, K., Krings, T., Borchardt, J., Kort, E. A., Sweeney, C., Conley, S., Roberts, D. A., and Dennison, P. E. Airborne DOAS retrievals of methane, carbon dioxide, and water vapor concentrations at high spatial resolution: Application to AVIRIS-NG. *Atmospheric Measurement Techniques*, 10(10):3833–3850, 2017. ISSN 18678548. doi: 10.5194/amt-10-3833-2017.

Varon, D. J., Jacob, D. J., McKeever, J., Jervis, D., Durak, B. O., Xia, Y., and Huang, Y. Quantifying methane point sources from fine-scale satellite observations of atmospheric methane plumes. *Atmospheric Measurement Techniques*, 11(10):5673–5686, 2018. ISSN 18678548. doi: 10.5194/amt-11-5673-2018.

Wang, J., Tchapmi, L. P., Ravikumar, A. P., McGuire, M., Bell, C. S., Zimmerle, D., Savarese, S., and Brandt, A. R. Machine vision for natural gas methane emissions detection using an infrared camera. *Applied Energy*, 257 (September 2019):113998, 2020. ISSN 03062619. doi: 10.1016/j.apenergy.2019.113998. URL https://doi.org/10.1016/j.apenergy.2019.113998.